Utility of Projective Geometry in Robot Localization

ARMIDA GONZÁLEZ LORENCE[1,2], MAYRA GARDUÑO G.[2] AND J. A. SEGOVIA DE LOS RÍOS[2,3]
[1] Instituto Tecnológico de San Juan del Río
Av. Tecnológico No. 2 CP. 76800, San Juan del Río, Querétaro, México

[2] Instituto Tecnológico de Toluca
Av. Inst. Tec. s/n, Metepec, Edo. México, México Tel. 01(722) 212-3197

[3] Instituto Nacional de Investigaciones Nucleares
Apdo. Post 18-1027, D. F. , México Tel. 01(55) 532-97-200

Abstract: - A very promising subject for robot localization is the vision area. However, this initiative has proved to be weak because the image is distorted due to the perspective view of the camera that captures such image and, therefore, it is impossible to improve the localization of the mobile robot that holds the camera. In this paper, we present a mobile robot localization vision system based on an innovative algorithm supported by the results of the strong analysis of diverse significant concepts of projective geometry. This way, the presence of a single landmark in the analyzed scene and the support of its perspective views offer a satisfactory absolute localization of the mobile robot carrying the camera.

1 Introduction

Several research works [3, 16, 24, 30] that intend to estimate the robot's localization based in vision techniques have proposed the use of three or at least two Artificial Landmarks as reference objects to improve the robot localization, but these Landmarks have to be distributed in an appropriate way to make an adequate localization [4, 17, 23]. However, due to the difficulty of properly selecting [1, 2] the landmarks involved in the localization process, other works have proposed combining these landmarks with other technologies like sonars [8, 12, 6], laser range finders [10], ultrasonic and infrared sensors [15, 25, 26] or laser lines [20].

We used the ideas of the works previously mentioned to determine the localization of our mobile robot P2-DX [18] but, to avoid the problem of selecting three adequate landmarks [4, 17], our work only required a single passive landmark. It is impossible to obtain the robot's configuration without using more support or without merging several methods, like other works do [9, 22, 21]; this is the reason to study the projective geometric properties [27, 29, 13] of the landmark design and use them to obtain the adequate robot's localization.

This research also considers using the minimum possible energy to increase the robot's autonomy; therefore, it uses a sensor like a PTZ CCD camera (Charge Coupled Device) [9]. For this reason, a robust landmark design was made so it could always be identified by the visual system, with several constant properties independent from the perspective view of the captured image.

2 Geometric-Projective Properties Used

Euclidean Geometry accurately describes the three-dimensional world. In this geometry, sides of objects have lengths, intersecting lines determine the angles between them and two lines are parallel if they lie in the same plane and never meet; these properties experience no modification with Euclidian transformations [11, 29]. However, when working with perspective views of the image process of a camera, lengths and angles change and parallel lines may intersect.

In fact, the Euclidian Geometry is only a subset of the Projective Geometry, which adequately models the imaging process because there are no lengths, angles or parallelism preserved, but projective transformations keep types (points remain points and lines remain lines), incidence (whether a point lies on a line) and also the measure called Cross Ratio [27, 13].

The Cross Ratio is a ratio or ratios of distances; it is always preserved and therefore becomes a very useful concept for our project. If there are four collinear points p_1, p_2, p_3 and p_4 where the Euclidean distance between two points p_i and p_j is denoted as Δ_{ij}, then the definition of the cross ratio appears in equation 1.

$$Cr(p_1, p_2; p_3, p_4) = \frac{\Delta_{13}\Delta_{24}}{\Delta_{14}\Delta_{23}} \tag{1}$$

To improve the Cross Ratio, point p_1 must be chosen as a reference point and then, the ratio of distances from that point p_1 to two other points p_3 and p_4 must be calculated; then, the ratio of distances from the remaining point p_2 to the same two points p_3 and p_4 must be computed. The ratio of these ratios is invariant under projective transformations.

The Euclidean distance between two points $p_i = [X_i, Y_i, Z_i]^T$ and $p_j = [X_j, Y_j, Z_j]^T$ is computed from the 2D Euclidean points (equation 2) obtained by dividing by the third coordinate:

$$\Delta_{ij} = \sqrt{\left(\frac{X_i}{Z_i} - \frac{X_j}{Z_j}\right)^2 + \left(\frac{Y_i}{Z_i} - \frac{Y_j}{Z_j}\right)^2} \quad (2)$$

The Cross Ratio is the same regardless of which coordinate is used as divisor (but always the same). However, the value of the Cross Ratio is different depending on the order chosen for the points involved, but once one order is selected, the Cross Ratio is always the same for that specific order.

Not surprisingly, since lines and points are dual, there is an equivalent Cross Ratio for lines defined on four lines which are incident in a single point, also called pencil of lines [27]; this may be computed by replacing the Euclidean distance between two points with the sine of the angle between lines. The cross ratio for lines will be the same regardless of the line used as reference, but once an order between the lines is selected, it must be kept as in the cross ratio for points.

It is important to know this. It is not necessary to have collinear original points. For example, given five points in a star configuration, as shown in the figure below, we can make four lines to evaluate the cross ratio by connecting the dots as shown in figure 1 (a); another possibility is to draw such lines starting from one of the points to the other four, as shown in figure 1 (b). In both cases, four concurrent lines whose cross ratio can be used are acquiescent.

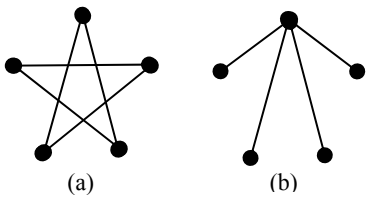

Fig. 1. Different configurations of lines to improve the Cross Ratio

The cross ratio of lines is defined in terms of the angles between the four lines (see equation 3).

$$Cr(l_1, l_2, l_3, l_4) = \frac{\sin\alpha_{13}\,\sin\alpha_{24}}{\sin\alpha_{23}\,\sin\alpha_{14}} \quad (3)$$

Many areas of the computer vision have little to do with the projective geometry, such as texture analysis, color segmentation and edge detection, and even in a field such as motion analysis, projective geometry offers little help because the relationship between the projection rays in successive images cannot be described by such simple mathematics.

But in areas such as camera calibration, stereo, object recognition, scene reconstruction mosaicing and image synthesis, projective geometry is a mathematical framework of great importance in computer vision.

However, in this work, properties of the projective geometry in the navigation processes of a mobile robot are applied. These properties are used to evaluate the localization of our robot with respect to one artificial landmark of well-known properties; involving the projective geometry cross ratio property in the localization process best identifies those properties. By using that property, it is possible to identify the actual position of the characteristic landmark points.

3 Properties of the Landmark

The design of the artificial landmark proposed (see figure 2) was initially inspired by the work presented in [24]; we are also considering that [16] mentions that "if the landmark characteristics are efficiently recognized, then the artificial landmarks can develop an impressive geometric localization".

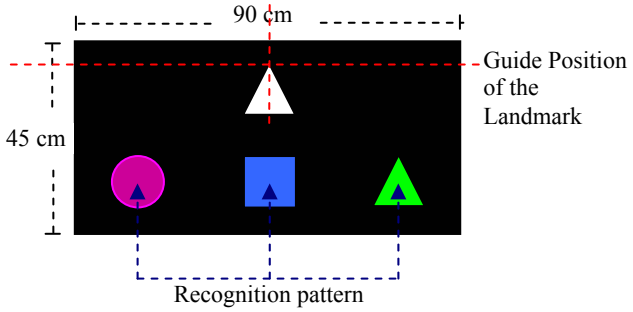

Fig. 2. Artificial landmark design, pattern figures area=63 cm^2 each, Euclidian distance between pattern figures centroids=23 cm.

The landmark's general color is black, easily recognizable in an office environment; the rectangular-shaped landmark is deformed when appreciated from a perspective view [11, 27, 29, 28, 13].

The landmark size is adapted for easy identification and placement on flat surfaces (e. g. walls); it is tied to the horizontal vision field of the camera used and to the landmark location method used [23]. With all this, the robot's camera always sees, at least, one artificial landmark, enough for our localization method.

Each landmark contains a recognition pattern formed by a set of three geometric figures easily recognizable [21]; this pattern increases the reliability of the

landmark identification process due to its horizontal orientation and the proportion of its areas; it also helps to evaluate the robot's orientation with respect to the landmark [27, 29].

There is a database named "*Code Table*" with a one-to-one relation between each recognition pattern and a specific configuration (x, y, θ) of the associated metric map (see Fig. 2) to obtain the absolute configuration of the robot.

With this artificial landmark design, it is possible to correct odometer deviations [2, 5] that any mobile robot accumulates during its navigation process.

3.1 Extraction of the landmark properties

The Landmark has special properties that allow us to obtain the information shown in figure 3.

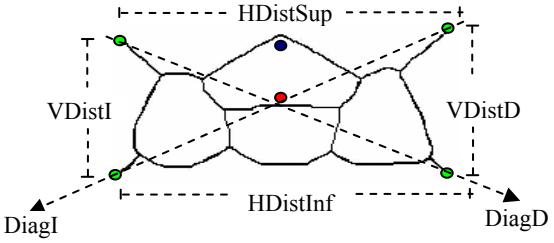

Position Guide	**HDistSup**	Superior vertical distance
Central point	**HDistInf**	Inferior vertical distance
Extreme points	**VDistI**	Left vertical distance
	VDistD	Right vertical distance
	DiagD	Right diagonal distance
	DiagI	Left diagonal distance

Fig. 3. Features extracted from the landmark

3.2 Association Landmark properties-Cross Ratio property

Previous to the mobile robot localization process, the camera is calibrated [21, 7] and the focal distance and the *r1*, *r2*, *r3* and *r4* distances to the landmark are evaluated. Distances *r1*, *r2*, *r3* and *r4* correspond to four vectors that go from the initial robot's configuration (0, 0, 0) to each point p_1, p_2, p_3 and p_4 of the landmark (see figure 4), the three vectors (the green vectors in figure 4) that converge on each point p_1, p_2, p_3 and p_4. are also evaluated here. Finally, the cross ratio of each group of green vectors that converge to *r1*, *r2*, *r3* and *r4* are also calculated.

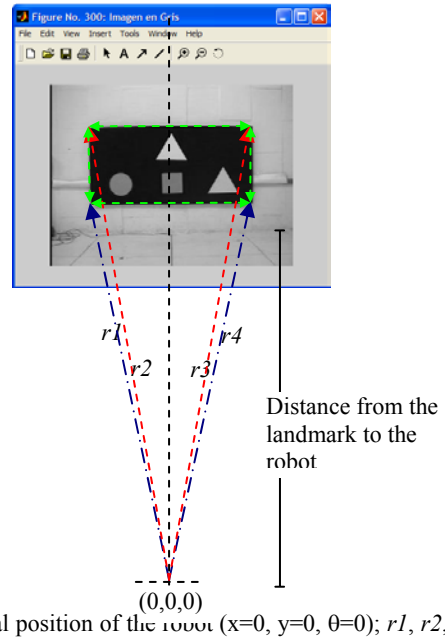

Fig. 4. Initial position of the robot (x=0, y=0, θ=0); *r1*, *r2*, *r3* and *r4* vectors

3.3 Orientation evaluation

Unlike the situation depicted in figure 4, where the robot's orientation coincides with the normal landmark, if the orientation angle changes, the view of the artificial landmark deforms (see figure 5); this information is used to evaluate the current robot's orientation with respect to the artificial landmark perceived at the moment.

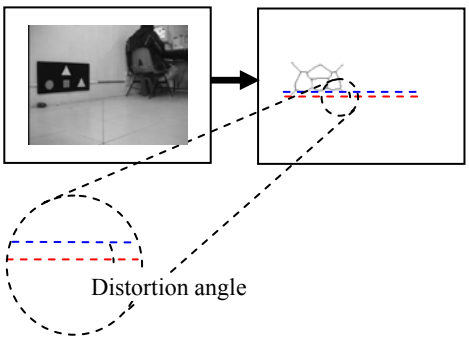

Fig. 5. Artificial landmark distortion

With the perspective landmark deformation, we obtain the information (*HDistSup*, *HDistInf*, *VDistI*, *VDistD*, *DistDiag* and *AngVision*) used in the localization algorithm to obtain the robot's orientation as illustrated in figure 6.

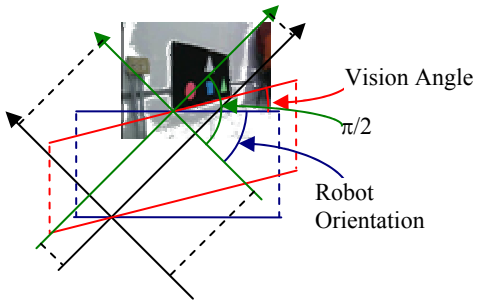

Fig. 6. Landmark perspective view with angle relation

3.4 Robot position evaluation

Figure 7 illustrates the geometric fundament of the algorithm. It is possible to recognize two triangular structures pointed toward vectors *r1* and *r3*, formed by both oriented segments: $r1=[p1,p2,p4,VDistI,HDistInf]$ and $r3=[p3,p2,p4,HDistSup,VDistD]$.

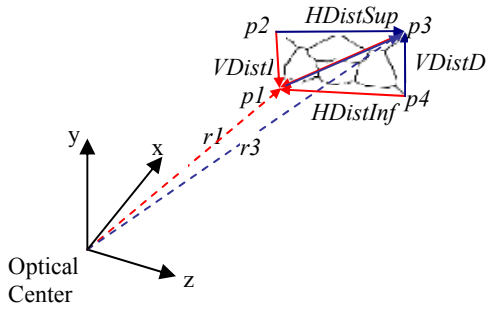

Fig. 7. Geometric fundament

With points p_1, p_2, p_3 and p_4 defined in the artificial landmark and admitting certain system restrictions, the solution sensibility notably decreases and increases the measure range of *r1*, *r2*, *r3* and *r4*. These restrictions essentially imply the "a priori" knowledge of the artificial landmark geometry and the restriction of the camera pan and tilt angles, both to 0.

The physical geometry of the landmark is well known. As specified in section 3 and mentioned before in section 3.1, the image landmark geometry was extracted, so, distances *VDistI*, *VDistD*, *HDistSup*, *HDistInf* and *DistDiag* and points p_1, p_2, p_3 and p_4 are known. If we apply the projective property Cross Ratio [27, 14, 28], where distance proportions are kept, we only have to deduce values *r1* and *r3* where we only know one of the points that constitute these distances; these points correspond to p_1 and p_3, respectively. The following algorithm derives from these considerations:

mr1= calculate_slope (p_1, UnknownLocation(x,y));
mVDistI= calculate_slope (p_1, p_2);
mDistDiag= calculate_slope (p_1, p_3);
mHDistInf= calculate_slope (p_1, p_4);
ang_r1_DistDiag= calculate_ang(r1,DistDiag);
ang_VDistI_HDistInf= calculate_ang(VDistI,HDistInf);
ang_VDistI_HdistDiag= calculate_ang(VDistI,HDiag);
ang_r1_HDistInf= calculate_ang(r1,HDistInf);

These calculations are used to obtain the Cross Ratio of the pencil formed with lines *r1*, *VDistI*, *DistDiag* and *HDistInf*; the partial result up to this moment is presented in equation 4. Such result depends on the unknown values (x,y) that correspond to the camera location. Note that the remaining values are known.

$$Cr1=\frac{Sin\left(\tan^{-1}\left(\frac{mDistDiag-\frac{p1.y-y}{p1.x-x}}{1-\frac{p1.y-y}{p1.x-x}\times mDistDiag}\right)\right)\times Sin(\alpha(mDistVI\_mDistHI))}{Sin(\alpha(mDistVI\_mDistDiag))\times Sin\left(\tan^{-1}\left(\frac{mDistHI-\frac{p1.y-y}{p1.x-x}}{1-\frac{p1.y-y}{p1.x-x}\times mDistHI}\right)\right)} \quad (4)$$

After that, obtain the Cross Ratio of the pencil formed with lines *r3*, *VDistD*, *DistDiag* and *HDistSup* with the following calculations:

mr3= calculate_slope (p_3 , UnknownLocation(x,y));
mVDistI= calculate_slope (p_3 , p_1);
mDistDiag= calculate_slope (p_3 , p_2);
mHDistInf= calculate_slope (p_3 , p_4);
ang_r3_HDistSup= calculate_ang(r3,HDistSup);
ang_DistDiag_VDistD= calculate_ang(DistDiag,VDistD);
ang_DistDiag_HDistSup= calculate_ang(DistDiag,HDistSup);
ang_r3_VDistD= calculate_ang(r3,VdistD);

Again, a partial result presented in equation 5 is obtained; this result also depends on the unknown values (x,y) that correspond to the camera location; the remaining values are known.

$$Cr3=\frac{Sin\left(\tan^{-1}\left(\frac{mDistHS-\frac{p1.y-y}{p1.x-x}}{1-\frac{p1.y-y}{p1.x-x}\times mDistHS}\right)\right)\times Sin(\alpha(mDisDiag\_mDistVD))}{Sin(\alpha(mDistDiag\_mDistHS))\times Sin\left(\tan^{-1}\left(\frac{mDistVD-\frac{p1.y-y}{p1.x-x}}{1-\frac{p1.y-y}{p1.x-x}\times mDistVD}\right)\right)} \quad (5)$$

Equation 5 represents the cross ratio of the pencil of lines that forms the upper triangle of figure 7; besides, as previously mentioned, values Cr1 and Cr3 are known because they were obtained after the calibration process; therefore, if we replace these known values in both equations (equations 4 and 5), there are two equations (4 and 5) with just two unknown values (x and y). If these two equation systems of two variable values are solved, it is possible to obtain the real values x and y

that correspond to the position of the robot's camera with respect to the artificial landmark.

4 Empirical Results

Figure 8 shows a sample of thirteen selected results that compare the real physical measures of mobile robot localization and the mobile robot localization obtained by means of this new algorithm.

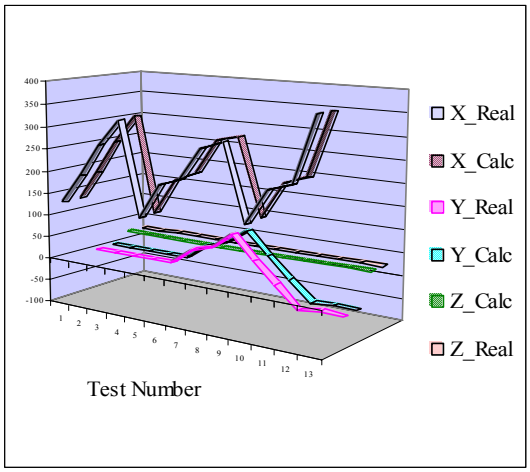

Fig. 8. Graphical representation of results obtained in selected tests

5 Conclusions

We can clearly see that the artificial landmarks proposed in several works require at least three landmarks to calculate a single data or "the current location of the robot". Therefore, these landmarks have demonstrated their weakness.

In this work, we assumed that image distortion has relevant importance to successfully recognize symbols and figures; furthermore, we assumed the limited intelligence of current mobile robots and we increased it with proper concepts of the projective geometry of the robot's ability to recognize deformed figures by offering some knowledge of perspective perception.

An algorithm was created to locate a robot with artificial landmarks that use the deformation that figures obtain under perspective. The purpose was to make the mobile robot enhance the form of deformed figures and to recognize them, just as human beings do.

We believe our efforts are worthy, although some researchers think that artificial landmarks will become obsolete with the arrival of better computing technology. We think that symbols cannot be eliminated from our modern world; we rather think that more researchers must do works like this to increase the limited intelligence of robots and to enhance their ability to recognize our modern symbols; robots should recognize those symbols even if the symbols are observed in a deformed way, just like human beings do with their deduction ability.

6 Acknowledgments

The development of this work is supported by CosNet (Mexico) with scholarship 2002240P and by financial support in part of this work (project 639.02-03-PR). Other important part of this work is supported by ANUIES and CONACyT (Mexico) with project M01-M01.

References:

[1] Betke, M. Gurvits L., Mobile Robot Localization Using Landmarks. Transactions on Robotics And Automation, Vol. 13, No. 2, Pages 251-263 (1997)

[2] Borenstein J., Everett H. R., Feng L., Where am I? Systems and Methods for Mobile Robot Positioning, Edited and compiled by J. Borenstein (1996)

[3] Brigs A. J., Scharstein D., Abbott S. D., Reliable Mobile Robot Navigation from Unreliable Visual Cues, Proceedings of the Fourth International Workshop on Algorithmic Foundations of Robotics WARF'2000, Hanover NH. (2000)

[4] Burschka D., Geiman J., Hager G., Optimal Landmark Configuration for Vision-Based Control of Mobile Robots, Proceedings of ICRA 2003 Conference, Taipei, Taiwan. (2003)

[5] Chenavier F., Crowley L. J., Position Estimation for Mobile Robot Using Vision and Odometry. Proceedings of the 1992 IEEE International Conference on Robotics and Automation, pages 2588-2593, Nice, France (1992)

[6] Drumheller M., Mobile Robot Localization Using Sonar. IEEE Transactions on Pattern Analysis and Machine Intelligence vol. 9, no. 2, pages 325-332 (1987)

[7] Faugeras O. D., Toscani G., Camera Calibration for 3D Computer Vision, Proc. Int. Workshop on Machine Vision and Machine Intelligence (1987)

[8] Gutmann J. S., Fox D., An Experimental Comparison of Localization Methods Continued, Proceedings of the IEEE/RSJ International Conference on Intelligent Robots and Systems IROS'2002, Lausanne, Switzerland (2002)

[9] Gutmann J. S., Markov-Kalman Localization for Mobile Robots, Proceedings of the International Conference on Pattern Recognition ICPR'2002, Quebec, Canada (2002)

[10] Gutmann J. S., Weigel T., Nebel B., A fast, Accurate, and Robust Method for Self-Localization in Polygonal Environments Using

Laser Range Finders. Advanced Robotics Journal, vol. 14 no. 8, pages 651-668 (2001)
[11] Hartley, R., Zisserman A., Multiple View Geometry in Computer Vision, Cambridge University Press, UK (2000)
[12] Jang G., Kim S., Lee W., Kweon I., Self-Localization of Indoor Mobile Robots using Sonar and Color Landmarks, International Workshop on Intelligent Robots, Hanyang University, Korea (2002)
[13] Kanatani, K., Computational Projective Geometry, CVGIP-54, No. 3 (1991)
[14] Kanatani, K., Geometric Computation for Computer Vision, Oxford University Press (1992)
[15] Kleeman. L., Optimal Estimation of Position and Heading for Mobile Robots Using Ultrasonic Beacons and Dead-reckoning. Proceedings of the 1992 IEEE International Conference on Robotics and Automation, pages 2582-2587, Nice, France (1992)
[16] Livatino S., Madsen C. B., Autonomous Robot Navigation with Automatic Learning of visual landmarks. 7th International Symposium on Intelligent Robotic System SIRS'1999, pages 419–428, Coimbra Portugal (1999)
[17] Madsen C. B., Andersen C. S., Optimal Landmark Selection for Triangulation of Robot Position. Journal of Robotics and Autonomous Systems (1998)
[18] Pioneer 2/PeopleBot, Operations Manual v9 ActiveMedia Robotics. http://www.activmedia.com (2001)
[19] PTZ Robotics Camera for Pioneer 2DX manual v2. ActiveMedia Incorporated http://www.activmedia.com (1999)
[20] Ríos N., Triana R., Garduño M., Segovia J. A., Navigation of a Mobile Robot Using a Laser Line, Proceedings of the 3th International Symposium on Robotics and Automation, ISRA'2002, Toluca, México, México (2002)
[21] Romero F., Reconocimiento de Figuras Simples Obtenidas de una Imagen Digital, Instituto Tecnológico de Toluca, Tesis (1997)
[22] Romero L., Morales E., Sucar E., A Robust Approach to Solve the Global Localization Problem for Indoor Mobile Robots Considering Sensor's Perceptual Limitations. Proceedings of the 3th International Symposium on Robotics and Automation, ISRA'2002, Toluca, México (2002)
[23] Salas J., Gordillo J. L., Placing Artificial Visual Landmarks in a Mobile Robot Workspace, IBERAMIA'1998, LNAI 1484, pages 274–282, Springer-Verlag Berlin Heidelberg (1998)
[24] Segovia A., Garduño M., Díaz A., Romero F., Sistema de Navegación de un Robot Móvil en Interiores, 1er. Congreso de Robótica, Asociación Mexicana de Robótica, A. C. AMRob, Torreón Coahuila México (1999)
[25] Segovia A., Martínez L., Alanís J., TRASMAR: A Semi-Autonomous Robot for Irradiated Materials Transportation. Proceedings of the 3th International symposium on Robotics and Automation ISRA'2002, Toluca, México (2002)
[26] Segovia A., Rivero T., Garduño M., Longoria C., Díaz A., Sistema Autónomo de Inspección. Las Perspectivas Tecnológicas de la Energía Nuclear y la Protección Radiológica para el Siglo XXI. Congreso Anual de la Sociedad Nuclear Mexicana. Reunión Anual de la Sociedad Mexicana de Seguridad Radiológica. Oaxaca, México (1998)
[27] Semple, J. G., Kneebone, G. T., Algebraic Projective Geometry, Oxford University Press (1952)
[28] Taubin G. Recognition and Positioning of rigid Object Using Algebraic and Moment Invariants, PhD. thesis, Brown University (1991)
[29] Verri A., Yuille A., Perspective Projection Invariants, MIT AI Memo 832, MIT (1986)
[30] Yoon K., Jang G., Kim S., Quejón I., Fast Landmark Tracking and Localization Algorithm for the Mobile Self-localization, IFAC Workshop on Mobile Robot Technology, pages 190-195 (2001)